Journal of Solid State Chemistry **157,** 160–165 (2001)
doi:10.1006/jssc.2000.9069, available online at http://www.idealibrary.com on IDEAL®

Crystal Structure of $Bi_{2.5}Me_{0.5}Nb_2O_9$ (*Me*= Na, K): A Powder Neutron Diffraction Study

Stefan Borg[1] and Göran Svensson

Department of Inorganic Chemistry, Chalmers University of Technology, SE-412 96 Göteborg, Sweden

Received August 4, 2000; in revised form December 4, 2000; accepted December 8, 2000

The room temperature structures of the two-layer Aurivillius phases $Bi_{2.5}Me_{0.5}Nb_2O_9$ (*Me* = Na, K) have been refined with the Rietveld method from powder neutron diffraction data ($\lambda = 1.470$ Å). They consist of $(Bi_2O_2)^{2+}$ layers interleaved with perovskite $(Bi_{0.5}Me_{0.5}Nb_2O_7)^{2-}$ (*Me* = Na, K) slabs. The structures were refined in the orthorhombic space group $A2_1am$, $Z = 4$, and the unit cell parameters of the two oxides are $a = 5.4937(3)$, $b = 5.4571(4)$, $c = 24.9169(14)$ Å and $a = 5.5005(8)$, $b = 5.4958(8)$, $c = 25.2524(16)$ Å, respectively. The orthorhombic distortion increases with decreasing Me^+ cation size in the perovskite layer $(Bi/Me)^{2+}$ site and the lone pair electrons from the Bi^{3+} cation are influencing the site distortion. This is in agreement with other two-layer Aurivillius phases and originates from bonding requirements depending on size and electronic environment.

Key Words: **Aurivillius phase; $Bi_{2.5}Na_{0.5}Nb_2O_9$; $Bi_{2.5}K_{0.5}Nb_2O_9$; powder neutron diffraction.**

INTRODUCTION

The first members of the Aurivillius phase family were discovered more than 50 years ago by B. Aurivillius when studying the Bi_2O_3–TiO_2 system. In four papers, published 1949–1952, he reported 14 new compounds within this family (1–4). About 10 years later the Aurivillius phase materials were recognized as possible ferroelectrics (5–7). At the end of the 1980s, after the discovery of the high T_c superconducting materials, there was an intensive search for other superconducting oxide systems. Despite the structural similarities with the Bi-based superconductors (8) no Aurivillius phase has yet showed any superconducting properties.

In recent years these complex metal oxides have been paid considerable attention since such materials possess properties usable for a variety of technical devices. The extensively investigated ferroelectric properties, with high transition temperatures and large spontaneous polarization (9), make it possible to use these materials as e.g. an information storage medium in nonvolatile computer memories (10). The ability of ion conductivity for some phases, with a given flux at a lower temperature comparable to that for other materials (11), as well as phases with catalytic properties for selective oxidation and ammoxidation (12), has broadened the range of possible applications.

In general, the composition of the Aurivillius phases can be formulated as $(M_2O_2)^{2+}(A_{m-1}B_mO_{3m+1})^{2-}$. *M* is usually occupied by Bi (13) and the oxides are hence built up by regular intergrowth of $(Bi_2O_2)^{2+}$ layers and perovskite $(A_{m-1}B_mO_{3m+1})^{2-}$ slabs. In the high-symmetry, nonpolar, tetragonal prototype structure, $I4/mmm$, the Bi atom binds to four oxygen atoms in a square pyramidal geometry. The *A* site is surrounded by 12 oxygen atoms in a dodecahedral coordination while the *B* atom occupies the BO_6 octahedra. This prototype structure is presumed to correspond to the crystal structure above the high-temperature phase transition. By transforming the $I4/mmm$ space group into a pseudotetragonal cell the undistorted $Fmmm$ parent structure is formed.

At room temperature the structure can be described by small orthorhombic or monoclinic deviations away from the undistorted $Fmmm$ parent structure leading to $a \neq b$. It has been customary to select the direction of spontaneous polarization along the *a*-axis and for compounds with *m* even the resultant lattice is *A*-centered. For $m = 2$ the space group has almost invariably been reported as $A2_1am$, which is a nonstandard settings of $Cmc2_1$ (14).

The spontaneous polarization in the ferroelectric phase of these types of materials is suggested to originate from several displacive mechanisms involving rigid displacements along the polar *a*-axis, as well as rotations around the *a*-axis and the *c*-axis (15). Not only the *B* site cations are displaced along the *a*-axis with respect to the oxygen octahedral framework but also the *A* site cations as well as the oxygen and the Bi ions in the $(Bi_2O_2)^{2+}$ layer. For compounds with $m = 2$ the contribution of the *A* site cations on the polarization varies with e.g. its electronic structure (16).

[1]To whom correspondence should be addressed. Fax: + 46 (0) 772 28 46. E-mail: borg@inoc.chalmers.se.

0022-4596/01 $35.00

The investigated oxides $Bi_{2.5}Me_{0.5}Nb_2O_9$ (Me = Na, K), with $m = 2$, were first reported by Aurivillius in 1949 (1). He described the structure in the space group *Fmmm* and was hence not able to observe the weak superstructure reflections. A phase diagram has been reported for the pseudobinary system $Bi_5Nb_3O_{15}$–$NaNbO_3$ including $Bi_{2.5}Na_{0.5}Nb_2O_9$ (17). Pham *et al.* (18) have synthesized the Aurivillius phase $Bi_2NaNb_2O_{8.5}$ with intrinsic oxygen vacancies for ionic conductivity measurements. They used X-ray powder diffraction for cell parameter refinement but did not refine any structure parameters. In this work the first structure refinements are reported with the *A* site containing a univalent cation as Na^+ or K^+.

Neutron powder diffraction has been used for the structure refinements since single crystals of Aurivillius phases of good quality for single-crystal diffraction are very difficult to grow because of e.g. twinning. Neutron diffraction does allow accurate determination of the oxygen positions in the presence of heavy atoms such as Bi.

EXPERIMENTAL

Polycrystalline, colorless samples of $Bi_{2.5}Me_{0.5}Nb_2O_9$ (Me = Na, K) were prepared by a two-step solid-state synthesis of stoichiometric quantities of Na_2CO_3 (Merck, $> 99.5\%$) or K_2CO_3 (Merck, $> 99\%$), Bi_2O_3 (Alfa, 99.975%), and Nb_2O_5 (Alfa, 99.9985%) powders, which were mixed and ground in ethanol before firing. The reactions took place in covered alumina crucibles in air, first at 800°C for 7 h as a powder. After regrinding and being pressed to pellets the samples were sintered at 1000°C for 10 h, cooled to 700°C at 30°C/h, and kept there for 7 h before being cooled to room temperature at the same rate.

To verify that no impurity phases were present in the samples, X-ray powder diffraction measurements were carried out on a Siemens D-5000 diffractometer. The measurements also showed that the samples demonstrated a high degree of crystallinity.

Neutron powder diffraction experiments were carried out at room temperature at the Swedish Research Reactor R2 in Studsvik. A thin-walled vanadium can of 10 mm in diameter was used as sample holder. The incident neutron beam wavelength was 1.470 Å, monochromated by two parallel copper crystals in the (220) mode. The reflection intensities were collected by means of a Huber two-circle diffractometer with an array of 35 ^{3}He detectors. The step scan covered the angular 2θ range 4.00–139.92° with a constant step size of 0.08°.

The structures were refined with the Rietveld method (19) in the space group $A2_1am$, using FullProf software (20). The neutron scattering lengths were taken from the program. Atomic coordinates reported by Ismunandar *et al.* (21) for $Bi_2SrNb_2O_9$ were used as the starting model in both refinements. The background intensities were described as a polynomial function of the fifth order and the peak shape was modeled by a pseudo-Voigt function. Peak asymmetry corrections were made for angles below 40° in 2θ. The *x* coordinate of the Bi(1)/Me (Me = Na, K) site in position 4*a* was held constant to establish an origin along the polar axis. The refinements were performed with a constant 50/50 molar distribution of Bi and Me in the Bi(1)/Me site. In the final cycles of refinement 47 parameters were varied for each sample, including 21 positional parameters and 8 isotropic displacement parameters. The diffraction patterns show a good agreement between the experimental data and the calculated profiles with no extra peaks observed in the patterns, see Figs. 1 and 2. The *R* factors along with the cell parameters and other refinement data are given in Table 1. The atomic coordinates and the isotropic displacement parameters are found in Table 2. A selection of bond distances calculated from the final coordinates is presented in Table 3.

RESULTS AND DISCUSSION

A perspective drawing of the oxide $Bi_{2.5}Na_{0.5}Nb_2O_9$ is shown in Fig. 3. Both investigated oxides $Bi_{2.5}Na_{0.5}Nb_2O_9$ and $Bi_{2.5}K_{0.5}Nb_2O_9$ consist of $(Bi_2O_2)^{2+}$ layers interleaved with perovskite $(Bi_{0.5}Me_{0.5}Nb_2O_7)^{2-}$ (Me = Na, K) slabs.

Examination of the bond distances in Table 3 shows that the coordination number for the Bi(1)/Me site can best be described as eight for both compounds according to the sum of effective ionic radii (22). Hence, it is not 12-coordinated as for the prototype structure in the $I4/mmm$ space group. The coordination around the site is more distorted for Me = Na than for Me = K due to the cation size.

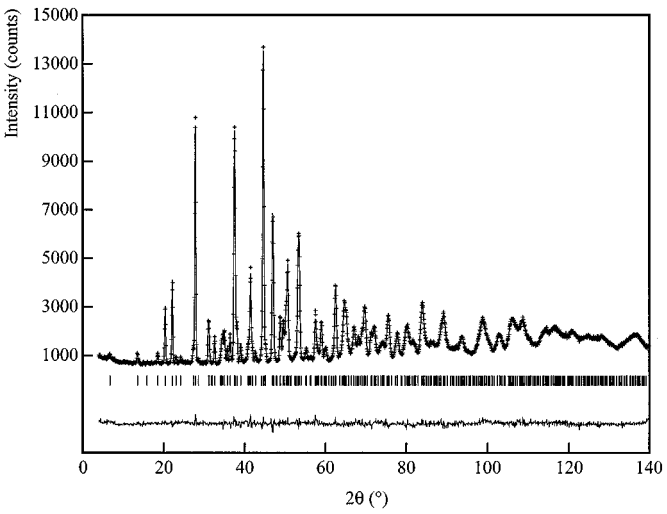

FIG. 1. Final Rietveld fit for $Bi_{2.5}Na_{0.5}Nb_2O_9$. Crosses represent observed data, and the solid line is the calculated pattern. The allowed Bragg reflection positions and the difference profile are shown beneath.

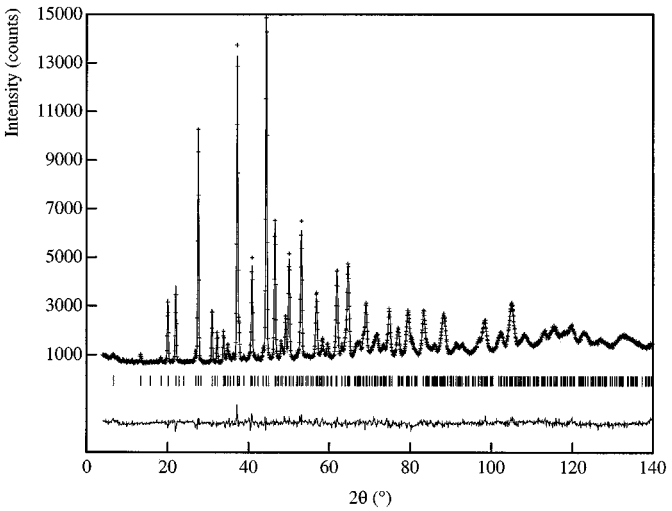

FIG. 2. Final Rietveld fit for $Bi_{2.5}K_{0.5}Nb_2O_9$.

Bond valence sums (23) associated with the different atom sites have been calculated and are presented in Table 4. The relationship between the length of a bond (r^{ij}) and its valence (s^{ij}) is $s^{ij} = \exp[(r_0^{ij} - r^{ij})/B]$, where r_0^{ij} and B are empirical parameters. The apparent bond valence V_i of atom i is then obtained as a sum over all the neighboring bond valences, i.e. $V_i = \sum_j s^{ij}$. It can be seen that the bond valence sum for Bi(1)/Na is almost 2 and thus they are satisfactorily bonded. For Bi(1)/K the bond valence sum is larger than two and hence "overbonding" occurs. Overbonding of the A site cation is common in two-layer Aurivillius phases with a divalent cation occupying the A site. The overbonding increases as the cation size increases (24). The bond valence sums are varying for the different oxygen sites and are in agreement with other $m = 2$ members of the Aurivillius phase family (25).

TABLE 1
Refinement Data

	$Bi_{2.5}Na_{0.5}Nb_2O_9$	$Bi_{2.5}K_{0.5}Nb_2O_9$
Formula weight	863.75	871.81
Crystal system	Orthorhombic	Orthorhombic
Space group	$A2_1am$	$A2_1am$
a (Å)	5.4937(3)	5.5005(8)
b (Å)	5.4571(4)	5.4958(8)
c (Å)	24.9169(14)	25.2524(16)
Volume (Å^3)	747.00(8)	763.37(17)
Z	4	4
D_x (Mg m^{-3})	7.679	7.585
No. of reflections	464	472
No. of data points	1700	1700
R_p (%)	2.99	3.60
R_{wp} (%)	3.90	4.71
R_{exp} (%)	2.50	2.55
R_B (%)	3.72	4.77
χ^2	2.44	3.42
No. of parameters	47	47

TABLE 2
Atomic Coordinates and Isotropic Displacement Parameters (Å^2)

Atom	Site	x	y	z	B
		$Bi_{2.5}Na_{0.5}Nb_2O_9$			
Bi(1)/Na	4*a*	0 [a]	0.2383(11)	0	0.84(12)
Bi(2)	8*b*	0.5067(14)	0.7283(6)	0.19938(9)	0.91(7)
Nb	8*b*	0.4591(12)	0.7459(9)	0.41549(9)	0.42(6)
O(1)	4*a*	0.4214(17)	0.1751(13)	0	0.53(12)
O(2)	8*b*	0.4439(16)	0.8059(9)	0.34220(13)	1.26(10)
O(3)	8*b*	0.7301(15)	−0.0047(8)	0.25040(18)	0.65(8)
O(4)	8*b*	0.6411(13)	0.9446(9)	0.08650(17)	0.63(9)
O(5)	8*b*	0.7235(17)	0.9697(9)	0.56709(15)	0.83(8)
		$Bi_{2.5}K_{0.5}Nb_2O_9$			
Bi(1)/K	4*a*	0 [a]	0.234(2)	0	0.7(2)
Bi(2)	8*b*	0.479(3)	0.7463(14)	0.20126(11)	1.47(9)
Nb	8*b*	0.463(3)	0.7490(17)	0.41260(11)	0.11(7)
O(1)	4*a*	0.445(3)	0.189(2)	0	1.5(2)
O(2)	8*b*	0.437(3)	0.7815(16)	0.34039(17)	1.18(13)
O(3)	8*b*	0.704(4)	−0.0026(16)	0.2499(4)	0.44(11)
O(4)	8*b*	0.665(3)	0.958(2)	0.0816(3)	2.0(2)
O(5)	8*b*	0.726(3)	0.9767(18)	0.5740(3)	1.13(14)

[a]Constrained to 0 to fix the origin along the a axis.

The stabilization of the perovskite layer by distortion of the Bi(1)/Me site requires the NbO_6 octahedra to tilt. The tilt can be described as rotations of the NbO_6 octahedra about the a and c axes where the neighboring octahedra rotate in opposite directions. For Me = Na and K the octahedral rotations about the a axis are 10.3° and 7.2° respectively, see Figs. 4a and 4b. The rotations about the c axis are of the same magnitude as for the a axis with 9.4° and 7.2°, see Figs. 4c and 4d. The rotations are effecting the orthorhombic distortion of the unit cell, which accordingly is greater for Na than for K as seen in Table 1. The mean Nb–O distance, 2.00(1) Å in both compounds, is in good agreement with the sum of their effective ionic radii, 2.04 Å (22). It is comparable to NbO_2, space group $I4_1/a$, with an average Nb–O bond distance of 2.05 Å and built up of NbO_6 octahedra sharing two sides (26). The niobium cations are slightly underbonded for both Aurivillius oxides and shifted away from the center of the octahedra, as seen in Fig. 4. The axial Nb displacement is smaller for Na than for K. The Nb cations are thus less displaced along the axial direction as the A cation size decreases, similar as for A = Ba, Sr, and Ca (24).

The Bi(2) atoms in the $(Bi_2O_2)^{2+}$ layers do not retain the four-fold coordination geometry in these samples as for the $I4/mmm$ prototype structure. Two additional bonds are

TABLE 3
Selected Bond Distances (Å)

	$Bi_{2.5}Na_{0.5}Nb_2O_9$	$Bi_{2.5}K_{0.5}Nb_2O_9$
	$(Bi_2O_2)^{2+}$ Layer	
Bi(2)–O(2)^{i}	2.550(6)	2.772(11)
Bi(2)–O(2)^{ii}	2.622(11)	2.73(2)
Bi(2)–O(2)^{iii}	3.266(11)	3.17(2)
Bi(2)–O(2)^{iv}	3.336(6)	3.133(11)
Bi(2)–O(2)	3.600(4)	3.526(5)
Bi(2)–O(3)^{iv}	2.165(8)	2.218(17)
Bi(2)–O(3)^{v}	2.290(8)	2.223(17)
Bi(2)–O(3)^{vi}	2.316(8)	2.368(18)
Bi(2)–O(3)^{vii}	2.490(8)	2.406(18)
Bi(2)–O(4)	3.138(5)	3.395(11)
	Perovskite layer	
Bi(1)–O(1)^{viii}	2.297(9)	2.348(18)
Bi(1)–O(1)	2.340(10)	2.46(2)
Bi(1)–O(1)^{ix}	3.198(10)	3.07(2)
Bi(1)–O(1)^{x}	3.231(9)	3.182(18)
Bi(1)–O(4)$^{vii,\ x}$	2.499(5) × 2	2.489(11) × 2
Bi(1)–O(4)$^{xi,\ xii}$	3.332(6) × 2	3.154(14) × 2
Bi(1)–O(5)$^{xiii,\ xiv}$	2.588(7) × 2	2.746(13) × 2
Bi(1)–O(5)$^{iii,\ xv}$	2.616(7) × 2	2.749(13) × 2
Nb–O(1)^{xvi}	2.151(3)	2.234(4)
Nb–O(2)	1.857(4)	1.838(6)
Nb–O(4)^{i}	1.925(8)	1.951(17)
Nb–O(4)^{iii}	2.033(9)	2.00(2)
Nb–O(5)^{xvii}	1.947(9)	1.94(2)
Nb–O(5)^{xviii}	2.067(9)	2.021(18)

Symmetry codes: (i) $x, y-\frac{1}{2}, \frac{1}{2}-z$; (ii) $\frac{1}{2}+x, \frac{3}{2}-y, \frac{1}{2}-z$; (iii) $x-\frac{1}{2}, \frac{3}{2}-y, \frac{1}{2}-z$; (iv) $x, \frac{1}{2}+y, \frac{1}{2}-z$; (v) $x, 1+y, z$; (vi) $x-\frac{1}{2}, \frac{1}{2}-y, \frac{1}{2}-z$; (vii) $x-\frac{1}{2}, 1-y, z$; (viii) $x-\frac{1}{2}, -y, -z$; (ix) $x-1, y, z$; (x) $x-\frac{1}{2}, 1-y, -z$; (xi) $x-1, y-1, -z$; (xii) $x-1, y-1, z$; (xiii) $x-1, y-\frac{1}{2}, \frac{1}{2}-z$; (xiv) $x-1, y-\frac{1}{2}, z-\frac{1}{2}$; (xv) $x-\frac{1}{2}, \frac{3}{2}-y, z-\frac{1}{2}$; (xvi) $x, \frac{1}{2}+y, \frac{1}{2}+z$; (xvii) $x, y, 1-z$; (xviii) $x-\frac{1}{2}, 2-y, 1-z$.

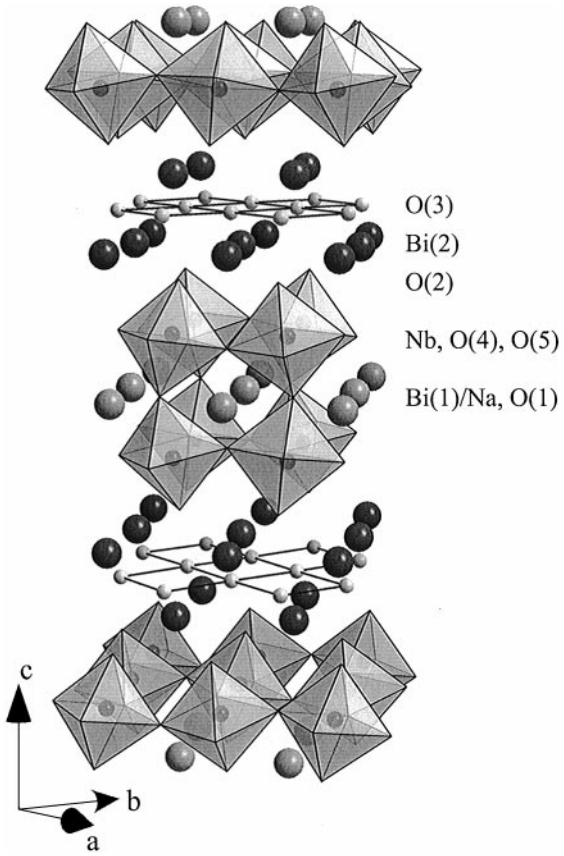

FIG. 3. Perspective drawing of $Bi_{2.5}Na_{0.5}Nb_2O_9$.

formed from the Bi(2) atom to two apex oxygens, O(2), from the tilting NbO_6 octahedra in the perovskite layer. These Bi(2)–O(2) bonds, 2.622(11), 2.550(6) Å for $Me = Na$ and 2.73(2), 2.772(11) Å for $Me = K$, are significantly longer than the four bonds that constitute the square pyramidal geometry with an average bond length of 2.315(8) and 2.304(19) Å, respectively. This will result in highly distorted polyhedra. The two remaining apex Bi(2)–O distances between 3.13(11) and 3.336(6) Å are considered as nonbonding according to the effective ionic radii. Such an anisotropically distorted geometry is characteristic for the stereochemical activity of the $6s^2$ lone pair electrons of the Bi^{3+} cations.

In order to estimate the influence of the *A* cation size for Aurivillius phases with $m = 2$ Camparnaud-Mesjard *et al.* (27) listed the unit cell parameters along with major components of the B_2O_7 octahedral framework distortion for the following phases: $Bi_2W_2O_9$ (27), $Bi_2CaNb_2O_9$ (24), Bi_3TiNbO_9 (28), $Bi_2SrNb_2O_9$ (21, 24), $Bi_2PbNb_2O_9$ (25), and $Bi_2BaNb_2O_9$ (21, 24). A general trend is that the distortion of the structure decreases with the increasing size of the *A* cation. The insertion of a voluminous cation in the site tends to regularize it and therefore minimize the tilt of the

TABLE 4
Bond Valence Sums (v.u.)

	$Bi_{2.5}Na_{0.5}Nb_2O_9$	$Bi_{2.5}K_{0.5}Nb_2O_9$
Bi(1)/Me^a	1.989	2.626
Bi(2)	2.990	2.831
Nb	4.923	4.973
O(1)	1.987	2.030
O(2)	1.881	1.784
O(3)	2.418	2.436
O(4)	2.122	2.267
O(5)	2.037	2.145

Empirical constants from Brown and Altermatt (23): $B = 0.37$, $r_0 = 2.094$ (Bi), 2.113 (Bi/K), 1.949 (Bi/Na), and 1.911 (Nb).
[a] $r_0(Bi(1)/Me) = (r_0(Bi) + r_0(Me))/2$.

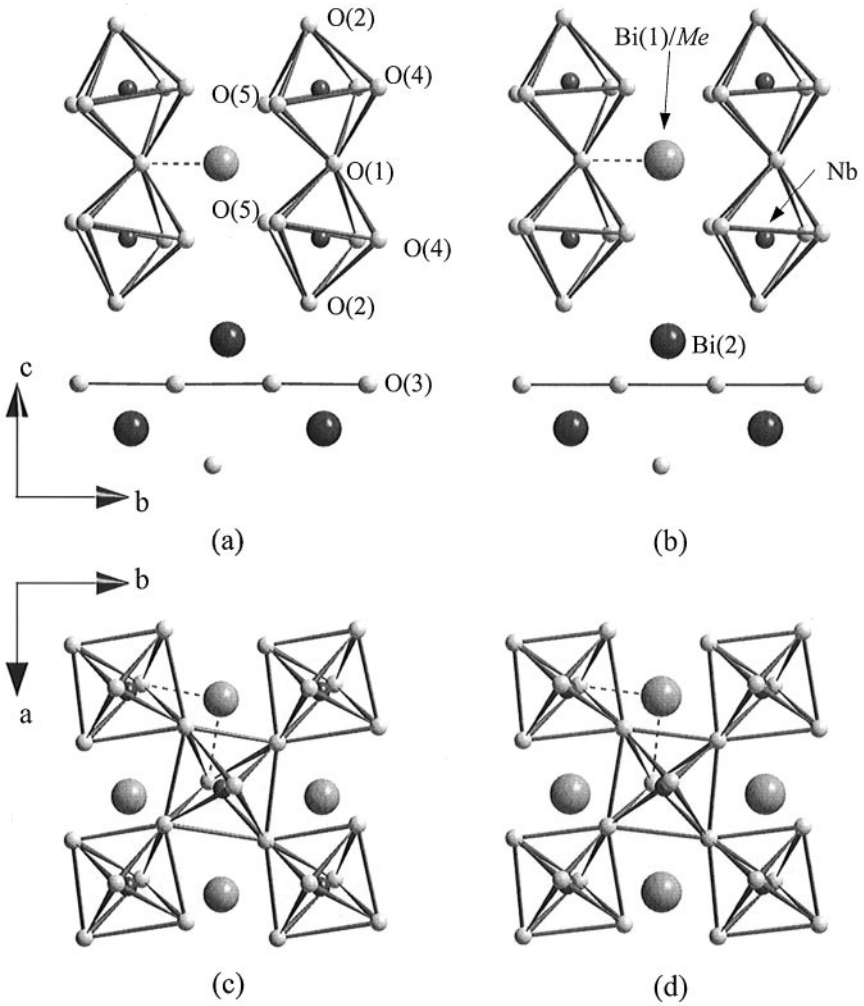

FIG. 4. Comparison of the distorted perovskite layers. Octahedra rotation about the *a* axis can be observed for (a) $Bi_{2.5}Na_{0.5}Nb_2O_9$ and (b) $Bi_{2.5}K_{0.5}Nb_2O_9$. The shortest Bi(1)/*Me* bonds are shown. In (c) and (d) the rotations about the *c* axis are viewed and the two shortest Bi(1)/*Me* bonds are indicated.

octahedra. The regularity is however broken for phases holding atoms with lone pair electrons like Bi^{3+} and Pb^{2+} in the *A* sites since there is a strong tendency to adopt a highly anisotropic coordination geometry. Two abnormally short bonds are formed with the axial O(1) atoms: 2.301(9) and 2.302(11) Å for Bi^{3+} and 2.35(3) and 2.43(3) Å for Pb^{2+}, compared to e.g., Sr^{2+} without lone pair electrons (2.53(2) and 2.58(2) Å).

In the investigated compounds the *A* sites are half filled with Bi^{3+} and the shortest Bi(1)/*Me*–O bonds, marked in Fig. 4, are 2.297(9) and 2.340(10) Å for Na along with 2.348(18) and 2.46(2) Å for K. The lone pair electrons from the Bi^{3+} cation are thus influencing the site distortion. When comparing the title compounds, in which the perovskite *A* site is holding atoms giving a fraction of lone pair electrons of 50%, with previously reported compounds (0 and 100% lone pair electrons), the distortion of the octahedra is increasing with increasing amount of lone pair contribution.

According to Camparnaud-Mesjard *et al.* (27) the strong *A*–O(1) bonds, for *A* cations with lone pairs, strengthen the rotation of octahedra around the *a* and *c* axes. This gives a decrease in the *a* and *b* parameters. The *c* parameter increases since the *B*–O(1) bonds instead are weakened, giving longer Nb–O(1) distances (2.26 and 2.28 Å for Bi^{3+} and Pb^{2+}).

For the investigated structures there is a decrease in the *a* and *b* parameters when *Me* = K but not when *Me* = Na. The *c* parameter increase does not agree with either $Bi_{2.5}Na_{0.5}Nb_2O_9$ or $Bi_{2.5}K_{0.5}Nb_2O_9$ and the Nb–O(1) distances of 2.151(3) and 2.234(4) Å are not exceptionally long.

ACKNOWLEDGMENTS

This work was supported by the Swedish Research Council for Engineering Sciences (TFR). The authors thank the Studsvik Neutron Research Laboratory (NFL) for neutron beam time and Håkan Rundlöf at NFL for collecting the neutron intensity data.

REFERENCES

1. B. Aurivillius, *Ark. Kemi* **1**(54), 463 (1949).
2. B. Aurivillius, *Ark. Kemi* **1**(58), 499 (1949).
3. B. Aurivillius, *Ark. Kemi* **2**(37), 519 (1950).
4. B. Aurivillius, *Ark. Kemi* **5**(4), 39 (1952).
5. G. A. Smolenskii, V. A. Isupov, and A. I. Agranovskaya, *Sov. Phys. Solid State* **1,** 149 (1959).
6. E. C. Subbarao, *J. Chem. Phys.* **34,** 695 (1961).
7. E. C. Subbarao, *J. Phys. Chem. Solids* **23,** 665 (1962).
8. R. L. Withers, J. G. Thompson, L. R. Wallenberg, J. D. Fitzgerald, J. S. Anderson, and B. G. Hyde, *J. Phys. C*: *Solid State Phys.* **21**(36), 6067 (1988).
9. L. Korzunova, *Ferroelectrics* **134**(1–4), 175 (1992).
10. J. F. Scott, F. M. Ross, C. A. Paz de Araujo, M. C. Scott, and M. Huffman, *Mater. Res. Soc. Bull.* **21**(7), 33 (1996).
11. K. R. Kendall, C. Navas, J. K. Thomas, and H. C. zur Loye, *Chem. Mater.* **8**(3), 642 (1996).
12. D. J. Buttrey, T. Vogt, U. Wildgruber, and W. R. Robinson, *J. Solid State Chem.* **111**(1), 118 (1994).
13. P. Millán, A. Castro, and J. B. Torrance, *Mater. Res. Bull.* **28**(2), 117 (1993).
14. "International Tables for Crystallography" (T. Hahn, Ed.), Vol. A, 2nd Ed. Reidel, Dordrecht, 1987.
15. R. L. Withers, J. G. Thompson, and A. D. Rae, *J. Solid State Chem.* **94,** 404 (1991).
16. A. D. Rae, J. G. Thompson, and R. L. Withers, *Acta Crystallogr. B* **48,** 418 (1992).
17. K. Homma, *J. Ceram. Soc. Jpn.* **97**(12), 1456 (1989).
18. A. Q. Pham, M. Puri, J. F. Dicarlo, and A. J. Jacobson, *Solid State Ionics* **72,** 309 (1994).
19. H. M. Rietveld, *J. Appl. Crystallogr.* **2,** 65 (1969).
20. J. Rodriguez-Carvajal, FULLPROF.98, Version 0.2, March 1998, Laboratoire Leon Brillouin (CEA/CNRS), CEA-Saclay, France, 1998.
21. Ismunandar, B. J. Kennedy, Gunawan, and Marsongkohadi, *J. Solid State Chem.* **126,** 135 (1996).
22. R. D. Shannon, *Acta Crystallogr. A* **32,** 751 (1976).
23. I. D. Brown and D. Altermatt, *Acta Crystallogr. B* **41,** 244 (1985).
24. S. M. Blake, M. J. Falconer, M. McCreedy, and P. Lightfoot, *J. Mater. Chem.* **7**(8), 1609 (1997).
25. V. Srikanth, H. Idink, W. B. White, E. C. Subbarao, H. Rajagopal, and A. Sequeira, *Acta Crystallogr. B* **52,** 432 (1996).
26. B.-O. Marinder, *Acta Chem. Scand.* **15,** 707 (1961).
27. J. C. Champarnaud-Mesjard, B. Frit, and A. Watanabe, *J. Mater. Chem.* **9**(6), 1319 (1999).
28. J. G. Thompson, A. D. Rae, R. L. Withers, and D. C. Craig, *Acta Crystallogr. B* **47,** 174 (1991).